Flow and heat transfer of a couple-stress fluid sandwiched between viscous fluid layers

J.C. Umavathi, A.J. Chamkha, M.H. Manjula, and A. Al-Mudhaf

Abstract: The problem of steady laminar fully developed flow and heat transfer in a horizontal channel consisting of a couple-stress fluid sandwiched between two clear viscous fluids is analyzed analytically. The fluids in all regions are assumed to be incompressible, immiscible, and the transport properties of the fluids in all regions are assumed to be constant. Under these assumptions, the resulting governing equations constitute a set of coupled linear ordinary differential equations that is solved analytically. The closed form solutions obtained for the velocity and temperature fields in the channel are evaluated numerically for various parametric conditions. These results are illustrated graphically to illustrate the effects of the physical parameters governing the flow such as the viscosity ratio, conductivity ratio, couple-stress parameter, Eckert number, and the Prandtl number on the velocity and temperature profiles. In addition, results for the rate of heat transfer are computed for different values of the physical parameters and presented in tabular form. It is found that the effect of the couple stress parameter is to promote the motion of the fluid.

PACS No.: 44.15.+a

Résumé : Nous proposons une étude analytique de l'écoulement laminaire complètement développé et le transfert de chaleur dans un canal horizontal consistant en un fluide à contrainte de couple (fluide polaire) entre deux fluides clairs visqueux. Tous les fluides sont présumés incompressibles, non miscibles et les propriétés de transport des fluides sont présumées constantes partout. Sous ces conditions, les équations décrivant le système forment un ensemble d'équations différentielles ordinaires linéaires que nous solutionnons analytiquement. Les champs de vitesse et de température ainsi obtenus sont évalués numériquement dans le canal horizontal pour différents ensembles des paramètres. Les résultats sont présentés graphiquement, afin d'illustrer les effets qu'ont les paramètres contrôlant l'écoulement sur les profils de vitesse et de température, comme le rapport de viscosité, le rapport de conductivité, le paramètre de contrainte de couple, le nombre de Eckert et le nombre de Prandtl. De plus, les taux de transfert de chaleur sont évalués pour différentes valeurs des paramètres physiques et présentés sous forme de tableau. Nous trouvons que l'effet du paramètre de contrainte de couple est d'améliorer le mouvement du fluide.

[Traduit par la Rédaction]

Received 17 June 2004. Accepted 31 March 2005. Published on the NRC Research Press Web site at http://cjp.nrc.ca/ on 13 July 2005.

J.C. Umavathi and M.H. Manjula. Department of Mathematics Gulbarga University, Gulbarga 585 106, India.
A.J. Chamkha[1] and A. Al-Mudhaf. Manufacturing Engineering Department, The Public Authority for Applied Education and Training, Shuweikh 70654, Kuwait.

[1]Corresponding author (e-mail: chamkha@paaet.edu.kw).

 doi: 10.1139/P05-032

1. Introduction

The theory of polar fluids was originally developed from a statistical mechanics model that assumed noncentral forces of interaction between particles. If the interparticle forces are not central forces in a particle–particle interaction there is an interparticle couple as well as an interparticle force; under the action of this couple, the fluid particles will have a tendency to rotate relative to their neighbours. The essential idea of a polar fluid is obtained by introducing a kinematic variable to model the forces that balance the action of the couple. Even though there is a slight simplification, it is the conceptual origin of the theory of polar fluids. Kinematically, the theory differs from other theories of fluid behavior, in that a particle angular velocity is defined independently of its velocity field and an axial vector field characterizing the rotational motion relative to the vorticity is constricted and the rotational motion of the fluid particles is considered to be proportional to the sum of these two independent fields. Mechanically, the polar fluid theory differs from other fluid theories in that angular momentum effects such as couple stresses and symmetry of the usually symmetric stress tensor are considered. The constitutive equations for polar fluids have been advanced from different view points by Cowin [1], Aero et al. [2] and Eringen [3]. They simply introduced the velocity and particle angular-velocity fields and postulated a dissipation function that leads to Grad's constitutive equations. Eringen [3] obtained the same constitutive equations by specializing his more general theory of microfluids Eringen [4]. Generalizations of the polar fluids are easy to construct using the director triad, which is required to remain rigid for polar fluids. The "theory of fluids with deformable microstructure" deals with fluid behaviour associated with a deformable director triad. This theory is discussed by Eringen [4] and Kline and Allen [5]. The more specialized theory of Eringen [6] called micropolar fluids with stretch is obtained by constraining the motion of the deformable triad so that all three directors remain perpendicular during the deformation and experience identical rates of length change. Both of these theories reduce to the polar fluid theory when the appropriate kinematical constraints on the driven triad are introduced. Finally, the theory of fluids with couple stresses is obtained if the polar fluid is constrained so that the Cosserat triad rotates with the underlying medium, but remains rigid. Thus, both polar and dipolar fluids reduce to the theory of fluids with couple stresses introduced by Stokes [7].

The couple-stress fluid model has wide applications in biofluids, colloidal fluids liquid crystals, and in engineering for pumping fluids such as synthetic lubricants. It is observed that slurries in general and animal blood in particular, show, under certain circumstances, strong deviation from a Newtonian fluid behavior. Initial studies of experimental data on blood, even though the data are by no means complete, lead us to believe that some deviations may be explained by assuming that blood is a fluid with couple stress. It is hoped that our paper will cast new light on blood behaviour and thus lead to more comprehensive experiments for the eventual understanding of the rheological properties of blood. Based on the couple-stress theory of Stokes [7], Valanis and Sun [8], Chaturani and Kaloni [9], and Chaturani and Upadthya [10] have proposed theoretical models for blood flow through narrow tubes. The theoretical results obtained from these three models are in good agreement with experimental results.

Further, Chaturani and Pralhad [11] studied a three-layered couette-flow model for blood flow and they assumed that the top and bottom layers consist of plasma (Newtonian fluid) and the middle layer consists of a red-cell suspension (couple-stress fluid). Recently, Malashetty and Umavathi [12] analyzed the effects of couple stresses on the free convective flow in a vertical channel. Free convection flow of an electrically conducting couple-stress fluid and a couple-stress fluid for the radiating medium in a vertical channel has been studied by Umavathi [13, 14]. Keeping in view the practical applications mentioned above, it is the objective of this paper to analyze the flow nature for couple-stress fluid sandwiched between clear viscous fluids

Fig. 1. Physical configuration.

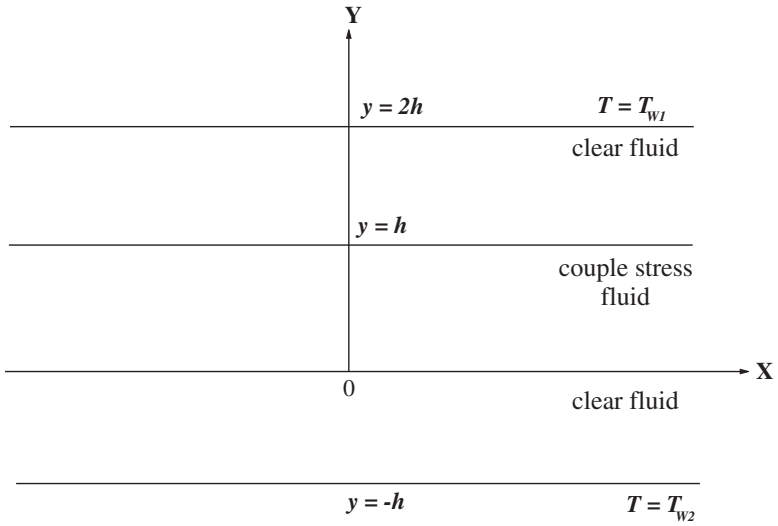

2. Mathematical formulation

The physical configuration (Fig. 1) consists of two infinite, horizontal parallel plates extending in the x- and z-directions. The flow and heat transfer in a system consists of a couple-stress fluid layer sandwiched between two viscous fluid layers. The regions $-h \leq y \leq 0$ and $h \leq y \leq 2h$ are filled with a clear viscous fluid of viscosity μ_1 and thermal conductivity K_1, and the region $0 \leq y \leq h$ is occupied by a couple-stress fluid having viscosity μ_2, thermal conductivity K_2, and a material constant η. The boundary walls of the channel are held at different constant temperatures, the upper wall is held at a temperature T_{W1} and the lower wall is held at a temperature T_{W2} with $T_{\mathrm{W1}} > {}_{\mathrm{W2}}$. The flow is assumed to be steady, laminar, and fully developed. Further, the fluid in all regions is assumed to be driven by a common constant pressure gradient $(-\partial P/\partial x)$ and that the existence of heat transfer does not affect the pressure gradient. The transport properties of the fluids in all regions are assumed to be constant.

Under these assumptions, the governing equations of motion and energy are

$$\chi_\mu \frac{\mathrm{d}^2 u_i}{\mathrm{d}y^2} - \chi \eta \frac{\mathrm{d}^4 u_i}{\mathrm{d}y^4} - \frac{\partial P}{\partial x} = 0 \tag{1}$$

$$\frac{\mathrm{d}^2 T_i}{\mathrm{d}y^2} + \chi_{\mu K} \left(\frac{\mathrm{d}u_i}{\mathrm{d}y} \right)^2 = 0 \tag{2}$$

where the subscript $i = 1, 2, 3$ gives the governing equations for Regions I, II, and III, respectively, and

χ_μ	=	μ_1	for a clear fluid region
	=	μ_2	for a couple stress fluid region
χ	=	0	for a clear fluid region
	=	1	for a couple stress fluid region
$\chi_{\mu K}$	=	$ac\mu_1/K_1$	for a clear fluid region
	=	$c\mu_2/K_2$	for a couple stress fluid region

where u is the x-component of the fluid velocity

and T is the temperature. The boundary conditions on velocity are the no-slip conditions and those on

the temperature are the isothermal conditions. The couple stresses vanish at the boundary, in addition, the continuity of velocity, shear stress, temperature, and heat flux at the two interfaces are assumed; also, the couple stresses vanish at the two interfaces (Valanis and Sun [8]).

The boundary and interface conditions on velocity are

$$u_1(2h) = 0, \qquad u_1(h) = u_2(h), \qquad u_2(0) = u_3(0), \qquad u_3(-h) = 0$$

$$\mu_1 \frac{\mathrm{d}u_1}{\mathrm{d}y} = \mu_2 \frac{\mathrm{d}u_2}{\mathrm{d}y} - \eta \frac{\mathrm{d}^3 u_2}{\mathrm{d}y^3} \quad \text{at} \quad y = h \tag{3}$$

$$\mu_2 \frac{\mathrm{d}u_2}{\mathrm{d}y} - \eta \frac{\mathrm{d}^3 u_2}{\mathrm{d}y^3} = \mu_1 \frac{\mathrm{d}u_3}{\mathrm{d}y} \quad \text{at} \quad y = 0$$

$$\frac{\mathrm{d}^2 u_2}{\mathrm{d}y^2} = 0 \quad \text{at} y = h, \qquad \frac{\mathrm{d}^2 u_2}{\mathrm{d}y^2} = 0 \quad \text{at} \quad y = 0$$

The boundary and interface conditions on temperature are

$$T_1(2h) = T_{\mathrm{W}1}, \qquad T_1(h) = T_2(h), \qquad T_2(0) = T_3(0), \qquad T_3(-h) = T_{\mathrm{W}2}$$

$$K_1 \frac{\mathrm{d}T_1}{\mathrm{d}y} = K_2 \frac{\mathrm{d}T_2}{\mathrm{d}y} \quad \text{at} \quad y = h \tag{4}$$

$$K_2 \frac{\mathrm{d}T_2}{\mathrm{d}y} = K_3 \frac{\mathrm{d}T_3}{\mathrm{d}y} \quad \text{at} \quad y = 0$$

Equations (1)–(4) are made dimensionless by using the following quantities:

$$u_i^* = \frac{u_i}{\bar{u}_1}, \qquad y^* = \frac{y}{h}, \qquad \theta = \frac{T - T_{\mathrm{W}2}}{T_{\mathrm{W}1} - T_{\mathrm{W}2}} \tag{5}$$

This yields

$$\chi \frac{\mathrm{d}^4 u_i}{\mathrm{d}y^4} - A_i \frac{\mathrm{d}^2 u_i}{\mathrm{d}y^2} = G_i \tag{6}$$

$$\frac{\mathrm{d}^2 \theta_i}{\mathrm{d}y^2} + F_i Ec Pr \left(\frac{\mathrm{d}u_i}{\mathrm{d}y} \right)^2 = 0 \tag{7}$$

where $i = 1, 2, 3$ gives the dimensionless equations for the Regions I, II, and III, respectively, and

$$A_1 = -1 = A_3, \qquad A_2 = \frac{a^2}{m}$$

$$G_1 = P = G_3, \qquad G_2 = -a^2 P$$

$$F_1 = 1 = F_3, \qquad F_2 = \frac{K}{m}$$

$$a^2 = \frac{\mu_1 h^2}{\eta}, \qquad Pr = \frac{\mu_1 C_P}{K_1}, \qquad Ec = \frac{\bar{u}_1^2}{C_P (T_{\mathrm{W}1} - T_{\mathrm{W}2})}$$

$$P = \frac{h^2}{\mu_1 \bar{u}_1} \left(\frac{\partial P}{\partial x} \right), \qquad m = \frac{\mu_1}{\mu_2}, \qquad K = \frac{K_1}{K_2}$$

The nondimensional form of the velocity, temperature boundary, and interface conditions reduce to

$$u_1(2) = 0, \qquad u_1(1) = u_2(1), \qquad u_2(0) = u_3(0), \qquad u_3(-1) = 0$$

$$\frac{du_1}{dy} = \frac{1}{m}\frac{du_2}{dy} - \frac{1}{a^2}\frac{d^3u_2}{dy^3} \quad \text{at} \quad y = 1 \tag{8}$$

$$\frac{du_2}{dy} - \frac{m}{a^2}\frac{d^3u_2}{dy^3} = m\frac{du_3}{dy} \quad \text{at} \quad y = 0$$

$$\frac{d^2u_2}{dy^2} = 0 \quad \text{at} \quad y = 1, \qquad \frac{d^2u_2}{dy^2} = 0 \quad \text{at} \quad y = 0$$

$$\theta_1(2) = 1, \qquad \theta_1(1) = \theta_2(1), \qquad \theta_2(0) = \theta_3(0), \qquad \theta_3(-1) = 0 \tag{9}$$

$$\frac{d\theta_1}{dy} = \frac{1}{K}\frac{d\theta_2}{dy} \quad \text{at} \quad y = 1, \qquad \frac{d\theta_2}{dy} = K\frac{d\theta_3}{dy} \quad \text{at} \quad y = 0$$

(The asterisks have been dropped for simplicity.)

3. Closed-form solutions

The governing equations of momentum and energy are linear ordinary differential equations and closed-form solutions can easily be obtained. Without going into detail, the solutions of (6) and (7) along with the boundary conditions given in (8) and (9) can be shown to be

$$u_1 = \frac{Py^2}{2} + C_1y + C_2 \tag{10}$$

$$u_2 = C_3 + C_4y + C_5\,\mathrm{Cosh}\,(A_4y) + C_6\,\mathrm{Sinh}\,(A_4y) + A_5y^2 \tag{11}$$

$$u_3 = \frac{Py^2}{2} + C_7y + C_8 \tag{12}$$

$$\theta_1 = r_1y^4 + r_2y^3 + r_3y^2 + B_1y + B_2 \tag{13}$$

$$\theta_2 = r_{14}\,\mathrm{Cosh}\,(2A_4y) + r_{15}\,\mathrm{Sinh}\,(2A_4y) + r_{16}y\mathrm{Cosh}\,(A_4y) + r_{17}y\,\mathrm{Sinh}\,(A_4y) + r_{18}\,\mathrm{Cosh}\,(A_4y) + r_{19}\,\mathrm{Sinh}\,(A_4y) + r_{20}y^4 + r_{21}y^3 + r_{22}y^2 + B_3y + B_4 \tag{14}$$

$$\theta_3 = r_{23}y^4 + r_{24}y^3 + r_{25}y^2 + B_5y + B_6 \tag{15}$$

3.1. Case 1

The solutions of (6) and (7) using the boundary conditions given by (8) and (9) in the absence of couple stresses are

$$u_1 = P\frac{y^2}{2} + C_1y + C_2 \tag{16}$$

$$u_2 = mP\frac{y^2}{2} + C_3y + C_4 \tag{17}$$

$$u_3 = P\frac{y^2}{2} + C_5y + C_6 \tag{18}$$

$$\theta_1 = B_1y + B_2 + r_1y^4 + r_2y^3 + r_3y^2 \tag{19}$$

$$\theta_2 = B_3y + B_4 + r_4y^4 + r_5y^3 + r_6y^2 \tag{20}$$

$$\theta_3 = B_5y + B_6 + r_7y^4 + r_8y^3 + r_9y^2 \tag{21}$$

3.2. Case 2

In the absence of couple stress and viscous dissipation, solution of (7) reduces to

$$\theta_i = \frac{(y+1)}{3} \qquad i = 1,\ 2,\ 3 \tag{22}$$

Since the velocity is independent of temperature, the solution of (6) remains the same as that of (16) in the absence of couple stresses and viscous dissipation.

4. Determination of viscosity of the couple-stress fluid

The viscosity of the couple-stress fluid is an important factor from the physiological as well as the engineering point of view (Dintenfass [15]). The shear viscosity μ_2 of the couple stress fluid can be determined by knowing the stress at any point.

$$\tau_i = \mu_i \frac{\mathrm{d}u_i}{\mathrm{d}y} \qquad i = 1, 2, 3 \tag{23}$$

Using (10) in (23), the viscosity of the couple-stress fluid μ_2 is obtained as

$$\mu_2 = \frac{\left(-Ph^2\mu_1 - 2h\mu_1\tau_3 + 2h\,\mu_1 Py\right)}{(-2hPy + 4h\tau_3)} \tag{24}$$

Since (τ_3, μ_1, h P) can be measured experimentally, one can evaluate μ_2 from (24). Stokes [7] method for the determination of the viscosity for a couple-stress fluid by a one-fluid model is valid only when the distance between the plates h is sufficiently large. But for small values of h, Stokes analysis may not be valid because suspensions have the tendency to leave a clear fluid layer near the walls. The method suggested by Chaturani and Upadthya [10] is quite involved, in that one has to first determine two other couple-stress parameters. The present method is a simple method and can be used to check the Chaturani and Upadthya method [10] considering the upper plate to be moving with V instead of no-slip velocity.

4.1. Rate of heat transfer

Apart from the velocity and temperature distribution in the channel, it is important to determine the rate of heat transfer between the plates and the fluid. The rate of heat transfer through the channel wall to the fluid is given by

$$Q = K\left(\frac{\partial T}{\partial y}\right)_{y=2h,-h} \tag{25}$$

The rate of heat transfer in dimensionless form can be written as

$$q = \left(\frac{\mathrm{d}\theta}{\mathrm{d}y}\right)_{\text{at } y=2,-1} \tag{26}$$

Based on the analytical solutions reported above, the rate of heat transfer at the top wall is given by

$$q_T = \left(\frac{\mathrm{d}\theta_1}{\mathrm{d}y}\right)_{\text{at } y=2} = 32r_1 + 12r_2 + 4r_3 + B_1 \tag{27}$$

while at the bottom wall, it is given by

$$q_B = \left(\frac{\mathrm{d}\theta_3}{\mathrm{d}y}\right)_{\text{at } y=-1} = -4r_{23} + 3r_{24} - 2r_{25} + B_5 \tag{28}$$

(The constants are defined in the Appendix).

Fig. 2. Velocity profiles for different values of the couple-stress parameter a.

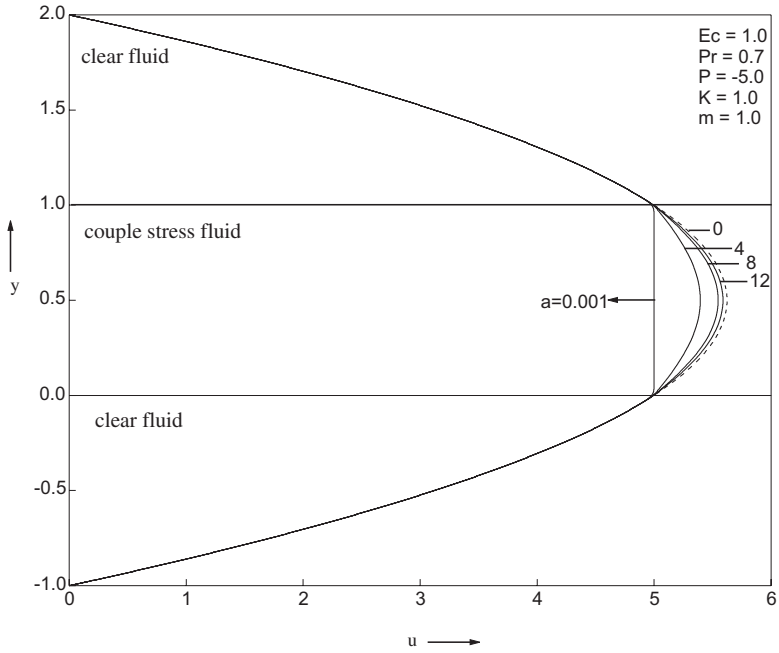

5. Results and discussion

Steady flow and heat transfer in a horizontal channel consisting of a couple-stress fluid layer sandwiched between two viscous fluid layers is studied. Closed-form solutions are obtained for the basic equations governing this flow situation. The closed-form solutions given by (10)–(15) are evaluated numerically for different values of the physical parameters and the results are presented graphically in Figs. 2–9.

The effect of the couple stress parameter a on the velocity profiles in the channel is shown in Fig. 2. It is observed from Fig. 2 that as the couple-stress parameter increases, the velocity increases. It is interesting to note that for sufficiently large values of a the velocity profile becomes almost unchanged. Hence, the flow can be stopped by choosing a large couple-stress parameter and on the other hand, the maximum flow rate can be achieved by choosing a small a small. Since a indicates the relation between the chain length of the molecules ($a = \frac{h}{l}$ where $l = \sqrt{\frac{\eta}{\mu_1}}$ is a function of molecular dimensions of the liquid) and distance between the plates, physically lower values of a correspond to larger values of the length of the polar additives. For example, the length of a polymer chain may be a million times the diameter of a water molecule. One might, therefore, expect couple stresses to appear in noticeable magnitudes in liquids with very large molecules. It is also seen from Fig. 2 that large values of a will lead to the flow nature being the same as that of a viscous fluid.

The effect of the viscosity ratio m on the velocity profiles is shown in Fig. 3. As the viscosity ratio increases, the velocity also increases and for large values of m, the velocity in the channel remains constant. Also, in the absence of couple stresses and as the viscosity ratio increases, the velocity increases, but it is more significant for $a = 0$

The effect of the couple-stress parameter a on the temperature profiles in the channel is shown in Fig. 4. As the couple-stress parameter increases, the temperature also increases in all regions and this increase is significant at the interfaces and in Region II. The temperature in the channel becomes almost

Fig. 3. Velocity profiles for different values of the ratio of the viscosities m.

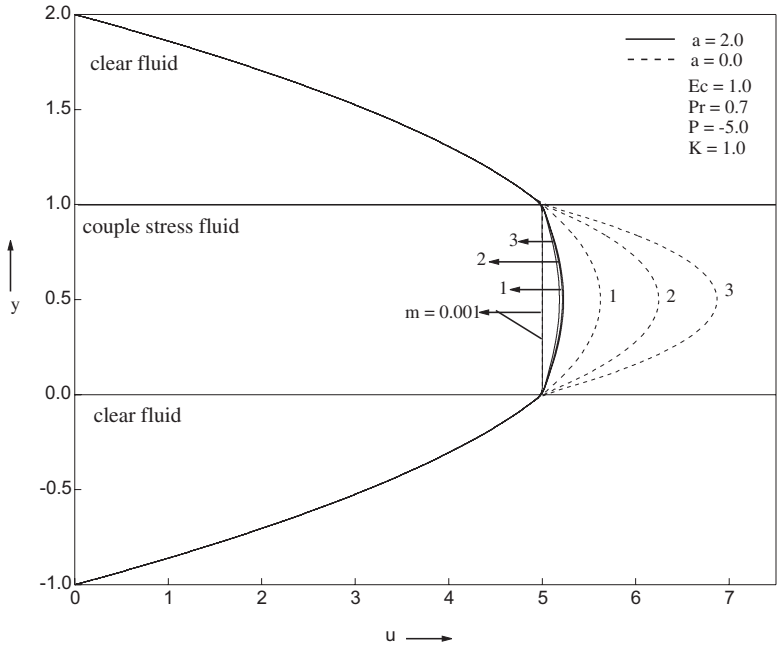

Fig. 4. Temperature profiles for different values of the couple-stress parameter a.

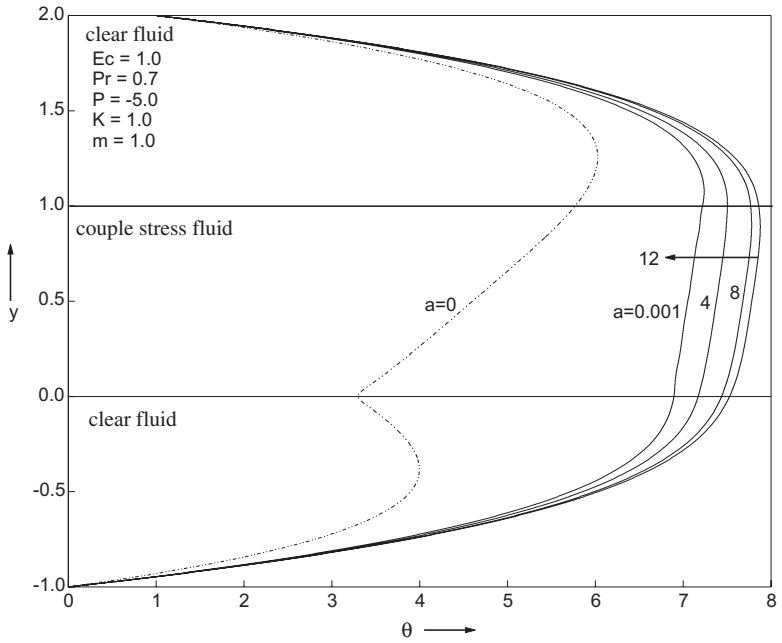

unchanged as a increases further and further. It is also observed that in the absence of couple stresses, the temperature profile is parabolic in Regions I and III and is linear in Region II. Since the temperature at the top plate is higher than the bottom plate, the temperature decreases from top to bottom. The effect

Fig. 5. Temperature profiles for different values of the ratio of the viscosities m.

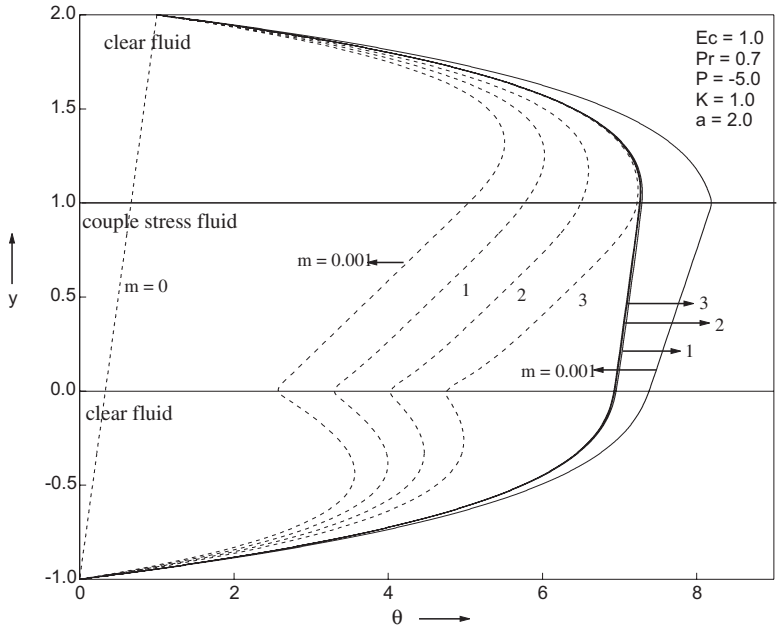

Fig. 6. Temperature profiles for different values of the ratio of the thermal conductivity K.

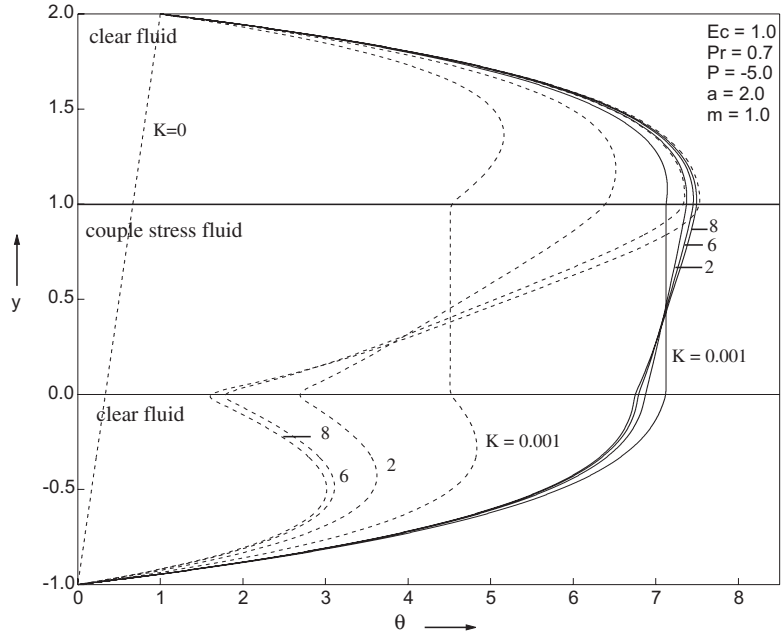

of the viscosity ratio m on the temperature profile is shown in Fig. 5. As the viscosity ratio increases, the temperature decreases. One can observe that for values of $m < 1$, the suppression in the temperature field is large compared to $m > 1$. Here also, the temperature attains a constant value for large m. In

Fig. 7. Temperature profiles for different values of the Eckert number Ec.

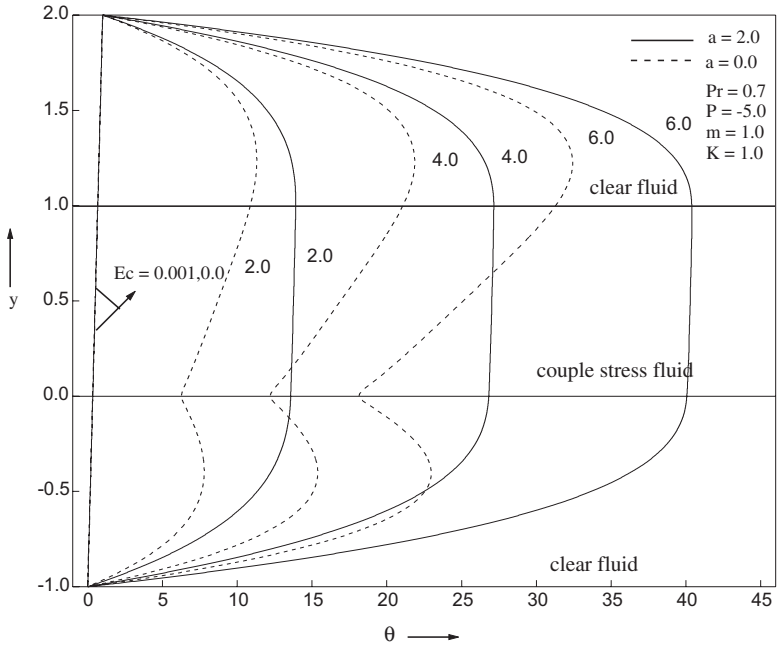

the absence of couple stresses, the temperature increases as the viscosity ratio increases, which is in contrast in the presence of couple stresses.

Figure 6 displays the effect of the conductivity ratio K on the temperature field. The temperature in the channel increases as K increases above $y = 0.448\,36$ and decreases below $y = 0.448\,36$. In the absence of couple stresses also the temperature increases as K increases above $y = 3.882\,32$ and decreases below $y = 3.882\,32$.

Figures 7 and 8 display the effects of the Eckert number Ec and the Prandtl number Pr on the temperature profiles in the channel. As either the Eckert number or the Prandtl number increases, the temperature in the channel increases, but the temperature profiles remain parallel to the y-axis for the couple-stress fluid region. As the Eckert number or Prandtl number increases, the temperature also increases in the absence of couple stresses, but the profiles are parabolic in Regions I and III and linear in Region II. The profile is linear in all the regions in the absence of Eckert and Prandtl numbers. The velocity profiles are shown in Fig. 9 for different values of shear viscosity μ_2 of the couple-stress fluid. In the present analysis the shear viscosity μ_2 of the couple-stress fluid is taken in the form $(\mu_1 + \mu_R)$ where μ_1 is the viscosity of the solvent fluid and μ_R is rotational viscosity. (The values of μ_R are taken from Ariman et al. [16] for 10% and 40% concentration). The numerical values of the velocities were computed from (1) using the boundary and interface conditions from (3) for different values of the concentration and layer thicknesses and are shown in Fig. 9. Since the velocity remains unchanged for the layer thickness in Regions I and III, the graph is drawn only for Region II. It is interesting to note that velocity decreases as the concentration increases, which is similar to the result obtained by Chaturani and Pralhad [11] in the upper half of the layer thickness. The effect of rotational viscosity for different solvent viscosity is shown in Table 1. It is observed that for solvent $\mu_1 < 1$, as the rotational viscosity μ_R increases the velocity decreases considerably. It can be seen that for $\mu_1 = 13$, there is not much variation in the velocity as μ_R increases.

The variation of the rate of heat transfer with different physical parameters is given in Table 2. We

Fig. 8. Temperature profiles for different values of the Prandtl number Pr.

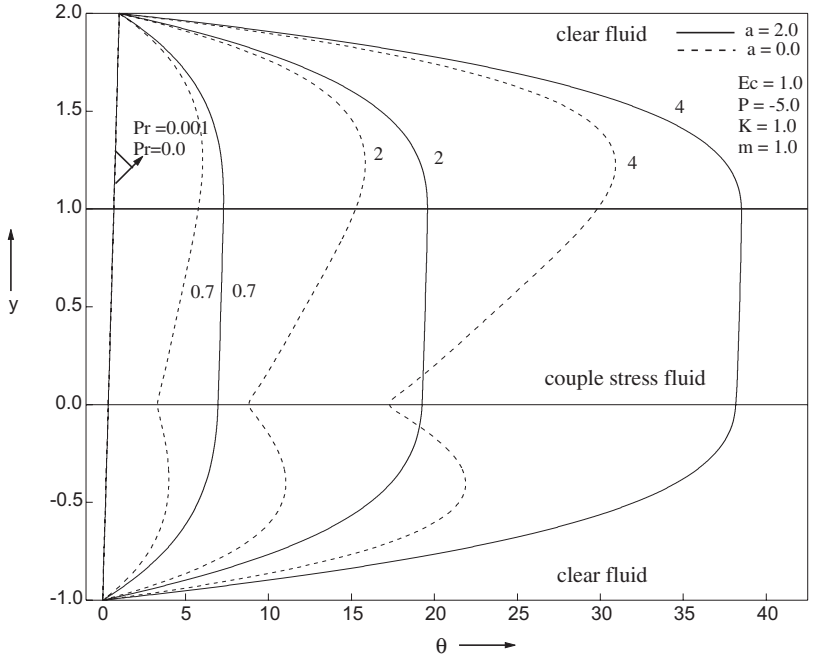

Fig. 9. Variation of velocity with concentration.

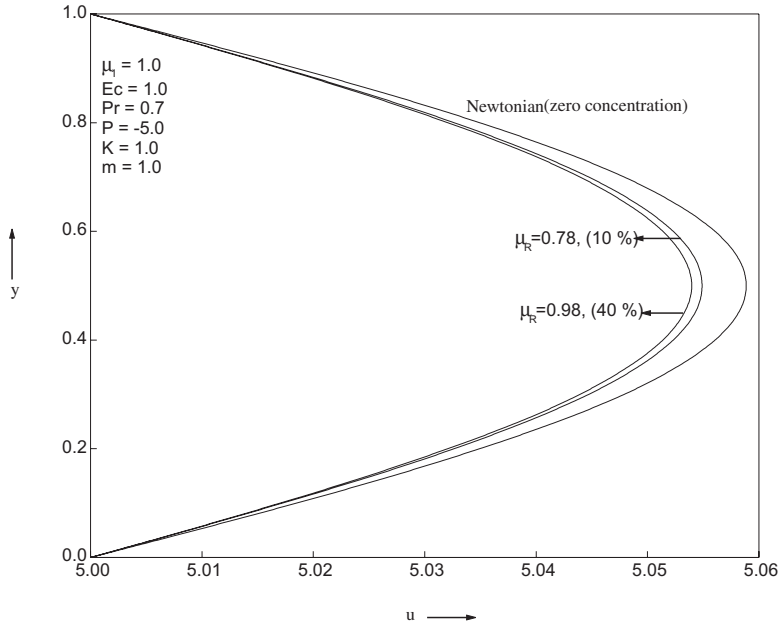

observe that as the viscosity ratio m increases, the rate of heat transfer increases for $m < 1$ and decreases for $m > 1$ at both walls of the channel. Increasing the values of the Eckert number and the Prandtl

Table 1. The variation of rotational viscosity μ_R for different solvent viscosity μ_1 on velocity of the couple-stress fluid.

	$\mu_R = 0.0$	$\mu_R = 0.78$	$\mu_R = 0.98$	$\mu_R = 0.0$	$\mu_R = 0.78$	$\mu_R = 0.98$
Y	$\mu_1 = 0.00018$ (air)			$\mu_1 = 0.0114$ (water)		
1.00	5.000000	4.999423	4.999541	5.000000	5.000000	5.000000
0.95	5.009424	4.999479	4.999586	5.009424	5.001357	5.001119
0.90	5.018577	4.999533	4.999628	5.018577	5.002655	5.002186
0.85	5.027217	4.999583	4.999668	5.027217	5.003852	5.003168
0.80	5.035130	4.999631	4.999706	5.035130	5.004922	5.004041
0.75	5.042133	5.000103	4.999742	5.042133	5.005846	5.004794
0.70	5.048072	5.000121	5.000019	5.048072	5.006613	5.005417
0.65	5.052822	5.000131	5.000103	5.052822	5.007216	5.005906
0.60	5.056283	5.000138	5.000110	5.056283	5.007649	5.006257
0.55	5.058388	5.000143	5.000114	5.058388	5.007911	5.006468
0.50	5.059094	5.000144	5.000125	5.059094	5.007998	5.006538
0.45	5.058388	5.000143	5.000114	5.058388	5.007911	5.006468
0.40	5.056283	5.000138	5.000110	5.056283	5.007649	5.006257
0.35	5.052822	5.000131	5.000104	5.052822	5.007216	5.005906
0.30	5.048072	5.000121	5.000096	5.048072	5.006613	5.005417
0.25	5.042133	5.000108	5.000086	5.042133	5.005846	5.004794
0.20	5.035130	5.000092	5.000073	5.035130	5.004922	5.004041
0.15	5.027216	5.000073	5.000058	5.027216	5.003852	5.003168
0.10	5.018577	5.000052	5.000041	5.018577	5.002655	5.002186
0.05	5.009424	5.000027	5.000022	5.009424	5.001357	5.001119
0.00	5.000000	5.000000	5.000000	5.000000	5.000000	5.000000
Y	$\mu_1 = 0.2$ (paraffin oil)			$\mu_1 = 13.0$ (glycerine)		
1.00	5.000000	5.000000	5.000000	5.000000	5.000000	5.000000
0.95	5.009424	5.006967	5.006533	5.009424	5.009373	5.009360
0.90	5.018577	5.013725	5.012867	5.018577	5.018476	5.018450
0.85	5.027217	5.020091	5.018831	5.027217	5.027068	5.027031
0.80	5.035130	5.025909	5.024278	5.035130	5.034938	5.034889
0.75	5.042133	5.031045	5.029085	5.042133	5.041903	5.041844
0.70	5.048072	5.035392	5.033151	5.048072	5.047809	5.047742
0.65	5.052822	5.038862	5.036395	5.052822	5.052531	5.052457
0.60	5.056283	5.041387	5.038755	5.056283	5.055974	5.055895
0.55	5.058388	5.042921	5.040188	5.058388	5.058067	5.057985
0.50	5.059094	5.043435	5.040669	5.059094	5.058769	5.058686
0.45	5.058388	5.042921	5.040188	5.058388	5.058067	5.057985
0.40	5.056283	5.041387	5.038755	5.056283	5.055974	5.055895
0.35	5.052822	5.038862	5.036395	5.052822	5.052531	5.052457
0.30	5.048072	5.035392	5.033151	5.048072	5.047809	5.047742
0.25	5.042133	5.031045	5.029085	5.042133	5.041903	5.041844
0.20	5.035130	5.025909	5.024278	5.035130	5.034938	5.034889
0.15	5.027216	5.020091	5.018831	5.027216	5.027068	5.027031
0.10	5.018577	5.013725	5.012867	5.018577	5.018476	5.018450
0.05	5.009424	5.006967	5.006533	5.009424	5.009373	5.009360
0.00	5.000000	5.000000	5.000000	5.000000	5.000000	5.000000

Table 2. The variation of the rate of heat transfer with different physical parameters.

	q_T	q_B		q_T	q_B
m			K		
0.1	−0.4268	1.0935	0.1	−0.2845	1.2369
0.5	−0.4278	1.0945	0.5	−0.3607	1.1607
1.0	−0.4273	1.0940	1.0	−0.4273	1.0940
2.0	−0.4266	1.0932	2.0	−0.5107	1.0107
4.0	−0.4259	1.0926	4.0	−0.5940	0.9273
6.0	−0.4256	1.0923	6.0	−0.6357	0.8857
8.0	−0.4255	1.0922	8.0	−0.6607	0.8607
10.0	−0.4254	1.0921	10.0	−0.6773	0.8440
12.0	−0.4253	1.0920	12.0	−0.6892	0.8321
Ec			a		
0.1	0.2572	0.4094	0.1	−0.4250	1.0916
0.5	−0.0470	0.7136	0.5	−0.4250	1.0916
1.0	−0.4273	1.0940	1.0	−0.4252	1.0919
2.0	−1.1881	1.8547	2.0	−0.4273	1.0940
4.0	−2.7095	3.3762	4.0	−0.4360	1.1026
6.0	−4.2310	4.8976	6.0	−0.4427	1.1094
8.0	−5.7524	6.4191	8.0	−0.4466	1.1133
10.0	−7.2739	7.9405	10.0	−0.4489	1.1155
12.0	−8.7953	9.4620	12.0	−0.4503	1.1169
Pr					
0.1	0.2246	0.4420			
0.5	−0.2100	0.8767			
1.0	−0.7534	1.4200			
2.0	−1.8401	2.5068			
4.0	−4.0136	4.6803			
6.0	−6.1871	6.8538			
8.0	−8.3606	9.0273			
10.0	−10.5341	11.2008			
12.0	−12.7076	13.3743			

number increases the rate of heat transfer significantly at the top and bottom plates. This is due to the significant increases in the wall-temperature gradients as either Ec or Pr increases. Furthermore, the rate of heat transfer at both plates of the channel increases considerably for sufficiently large values of the couple stress parameter a. It is also observed that as the conductivity ratio K increases, the rate of heat transfer increases at the top plate and decreases at the bottom plate.

6. Conclusion

The problem of steady fully developed flow and heat transfer of a couple-stress fluid sandwiched between two layers of viscous Newtonian fluids through a horizontal isothermal parallel-plates channel under the action of a constant pressure gradient was studied. Closed-form solutions were obtained by solving the governing equations subject to the proper boundary and interface conditions. The analytical solutions for the velocity and temperature profiles in the three-layer regions were evaluated numerically and a parametric study illustrating the influence of the various physical parameters on the hydrodynamic

and thermal fields was conducted. The physical parameters governing the heat transfer characteristics such as the rate of heat transfer at the top and bottom walls of the channel were also evaluated for various conditions. The effect of increasing the couple-stress parameter was found to increase the velocity and temperature fields in the channel. Furthermore, the rate of heat transfer at both plates of the channel increased as the couple stress parameter was increased.

Acknowledgement

This work is supported by UGC-New Delhi under the Special Assistance Programme DRS. One of the authors M.H.M. thanks UGC for the financial assistance through SAP.

References

1. S.C. Cowin. Ph.D. thesis. The Pennsylvania State University, Penn. 1962.
2. E.L. Aero, A.N. Bullygin, and E.V. Kuvshinskii. Appl. Math. Mech. **333**, 29 (1963).
3. A.C. Eringen. J. Math. Mech. **16,** 1 (1966).
4. A.C. Eringen. Int. J. Eng. Sci. **2**, 205 (1964).
5. K.A. Kline, S.J. Allen, and C.N. Desilva. Biorheology, **5**, 111 (1968).
6. A.C. Eringen. Int. J. Eng. Sci. **7**, 115 (1969).
7. V.K. Stokes. Phys. Fluids. **9**, 1709 (1966).
8. K.C. Valanis and C.T. Sun. Biorheology, **6**, 85 (1969).
9. P. Chaturani and P.N. Kaloni. Biorheology, **13**, 243 (1976).
10. P. Chaturani and V.S. Upadthya. Biorheology, **16**, 109 (1979).
11. P. Chaturani and R.N. Pralhad. Biorheology, **12**, 283 (1981).
12. J.C. Umavathi and M.S. Malashetty. Int. J. Nonlinear Mech. **34**, 1034 (1999).
13. J.C. Umavathi. ASME. **68**(1), 1 (1999).
14. J.C. Umavathi. ASME. **69**(8), 1 (2000).
15. L. Dintenfass. Cardiovascular Med. **2,** 337 (1977).
16. T. Ariman, M.A. Turk, and N.D. Sylvester. J. Appl. Mech. **41**, 1 (1974).

Appendix A. Definition of constants

$$A_4 = \sqrt{A_2}, \qquad A_5 = \frac{-G_2}{2A_2}, \qquad A_6 = \frac{-EcPrK}{m}$$

$$B_1 = \frac{e_1 - e_7}{2 + K}, \qquad B_2 = e_1 - 2B_1, \qquad B_3 = KB_1 - e_5$$

$$B_4 = B_1 + B_2 - B_3 - e_2, \qquad B_5 = B_6 - e_4, \qquad B_6 = B_4 + e_3$$

$$C_1 = \frac{mD_5 - mD_3C_5 - mD_4C_6 + C_4}{m}, \quad C_2 = D_1 - 2C_1, \quad C_3 = C_8 - C_5, \quad C_4 = mC_7 - D_6C_6$$

$$C_5 = \frac{-2A_5}{A_4^2}, \qquad C_6 = \frac{-\left(2A_5 + A_4^2C_5\,\mathrm{Cosh}\,(A_4)\right)}{A_4^2\,\mathrm{Sinh}\,(A_4)}, \qquad C_7 = \frac{P + 2D_9}{2\,(1 + mD_8)}, \qquad C_8 = \frac{2C_7 - P}{2}$$

$$D_1 = -2P, \qquad D_2 = \frac{(2C_5\,\mathrm{Cosh}\,(A_4) + 2C_6\,\mathrm{Sinh}\,(A_4) + 2A_5 - P)}{2}$$

$$D_3 = \frac{mA_4^3\,\mathrm{Sinh}A_4 - a^2A_4\,\mathrm{Sinh}A_4}{ma^2}, \qquad D_4 = \frac{mA_4^3\,\mathrm{Cosh}A_4 - a^2A_4\,\mathrm{Cosh}A_4}{ma^2}$$

$$D_5 = \frac{(2A_5 - mP)}{m}, \qquad D_6 = \frac{\left(a^2A_4 - mA_4^3\right)}{a^2}$$

$$D_7 = (D_5 - D_3C_5 - D_4C_6)\,, \qquad D_8 = \frac{1+m}{m}, \qquad D_9 = D_1 - D_2 - D_7 + C_5 + D_6D_8C_6$$

$$e_1 = (1 - 16r_1 - 8r_2 - 4r_3)$$

$$e_2 = \left(\begin{array}{l} r_{14}\,\mathrm{Cosh}\,(2A_4) + r_{15}\,\mathrm{Sinh}\,(2A_4) + r_{16}\,\mathrm{Cosh}\,(A_4) + r_{17}\,\mathrm{Sinh}\,(A_4) \\ +r_{18}\,\mathrm{Cosh}\,(A_4) + r_{19}\,\mathrm{Sinh}\,(A_4) + r_{20} + r_{21} + r_{22} - r_1 - r_2 - r_3 \end{array} \right)$$

$$e_3 = r_{14} + r_{18}, \qquad e_4 = -\,(r_{23} - r_{24} + r_{25})$$

$$e_5 = \left(\begin{array}{l} 2A_4r_{14}\,\mathrm{Sinh}\,(2A_4) + 2A_4r_{15}\,\mathrm{Cosh}\,(2A_4) + A_4r_{16}\,\mathrm{Sinh}\,(A_4) \\ +r_{16}\,\mathrm{Cosh}\,(A_4) + A_4r_{17}\,\mathrm{Cosh}\,(A_4) + r_{17}\,\mathrm{Sinh}\,(A_4) + A_4r_{18}\,\mathrm{Sinh}\,(A_4) \\ +A_4r_{19}\,\mathrm{Cosh}\,(A_4) + 4r_{20} + 3r_{21} + 2r_{22} - 4Kr_1 - 3Kr_2 - 2Kr_3 \end{array} \right)$$

$$e_6 = (2A_4r_{15} + r_{16} + A_4r_{19})\,, \qquad e_7 = \frac{(Ke_2 - Ke_3 - Ke_5 - e_5 + e_6 + Ke_4)}{K}$$

$$r_1 = \frac{-EcPrP^2}{12}, \qquad r_2 = \frac{-EcPrPC_1}{3}, \qquad r_3 = \frac{-EcPrC_1^2}{2}$$

$$r_4 = A_6A_4^2C_5^2, \qquad r_5 = A_6A_4^2C_6^2, \qquad r_6 = A_6C_5C_6A_4^2$$

$$r_7 = 4A_6A_4A_5C_6, \qquad r_8 = 4A_6A_5A_4C_5, \qquad r_9 = 2A_6C_4C_6A_4$$

$$r_{10} = 2A_6C_4C_5A_4, \qquad r_{11} = 4A_6A_5^2, \qquad r_{12} = 4A_6A_5C_4$$

$$r_{13} = A_6C_4^2, \qquad r_{14} = \frac{(r_4 + r_5)}{8A_4^2}, \qquad r_{15} = \frac{r_6}{4A_4^2}$$

$$r_{16} = \frac{r_7}{A_4^2}, \qquad r_{17} = \frac{r_8}{A_4^2}, \qquad r_{18} = \left(\frac{-2r_8}{A_4^3} + \frac{r_9}{A_4^2} \right)$$

$$r_{19} = \left(\frac{-2r_7}{A_4^3} + \frac{r_{10}}{A_4^2} \right), \qquad r_{20} = \frac{r_{11}}{12}, \qquad r_{21} = \frac{r_{12}}{6}, \qquad r_{22} = \frac{2r_{13} + r_5 - r_4}{4}$$

$$r_{23} = \frac{-EcPrP^2}{12}, \qquad r_{24} = \frac{-EcPrPC_7}{3}, \qquad r_{25} = \frac{-EcPrC_7^2}{2}$$

Case 1

$$B_1 = \frac{(D_1 - D_5)}{(2+K)}, \qquad B_2 = D_1 - 2B_1, \qquad B_3 = KB_1 - D_4$$

$$B_4 = B_1 + B_2 - B_3 - D_2, \qquad B_5 = B_6 - D_3, \qquad B_6 = B_4$$

$$C_1 = \frac{-(2P + C_2)}{2}, \qquad C_2 = \frac{(-2Pm + Pm - 2P)}{(m+2)}, \qquad C_3 = C_1 + C_2 - C_4 - \frac{P}{2}(m-1)$$

$$C_4 = C_1 - \frac{P}{2}, \qquad C_5 = C_1, \qquad C_6 = C_4$$

$$D_1 = (1 - 16r_1 - 8r_2 - 4r_3)\,, \qquad D_2 = (r_4 + r_5 + r_6 - r_1 - r_2 - r_3)$$

$$D_3 = -\,(r_7 - r_8 + r_9)\,, \qquad D_4 = (4r_4 + 3r_5 + 2r_6 - 4Kr_1 - 3Kr_2 - 2Kr_3)$$

$$D_5 = D_2 - D_4 - \frac{D_4}{K}, \qquad r_1 = -\frac{EcPrP^2}{12}, \qquad r_2 = -\frac{EcPrPC_1}{3}, \qquad r_3 = -\frac{EcPrPC_1^2}{2}$$

$$r_4 = -EcPr\frac{K}{m}\frac{m^2P^2}{12}, \qquad r_5 = -EcPr\frac{K}{m}\frac{mPC_3}{3}$$

$$r_6 = -EcPr\frac{K}{2m}C_3^2, \qquad r_7 = -EcPr\frac{P^2}{12}, \qquad r_8 = -EcPr\frac{PC_5}{3}, \qquad r_9 = -EcPr\frac{C_5^2}{2}$$

List of symbols

$\left(\frac{\mu_1 h^2}{\eta}\right)$	a couple stress parameter
C_{P}	specific heat at constant pressure
Ec	Eckert number, $\left(\frac{\bar{u}_1^2}{C_{\mathrm{P}}(T_{\mathrm{W1}}-T_{\mathrm{W2}})}\right)$
h	height of the Regions I, II, and III
K	ratio of thermal conductivities, $\left(\frac{K_1}{K_2}\right)$
K_1	thermal conductivity of the fluid in Regions I and III
K_2	thermal conductivity of the fluid in Region II
m	ratio of the viscosities, $\left(\frac{\mu_1}{\mu_2}\right)$
P	nondimensional pressure gradient, $\left(\frac{h^2}{\mu_1 \bar{u}_1}\frac{\partial P}{\partial x}\right)$
Pr	Prandtl number, $\left(\frac{\mu_1 C_P}{K_1}\right)$
T	temperature
T_{W1}, T_{W2}	temperature of the boundaries
u	velocity
$\bar{u}_1$	average velocity
x, y	space coordinates

Greek symbols

η	material constant
θ	nondimensional temperature, $\left(\frac{T-T_{\mathrm{W2}}}{T_{\mathrm{W1}}-T_{\mathrm{W2}}}\right)$

Subscripts

1, 2, and 3	quantities for Regions I, II and III, respectively.